



# A RANDOM FIBRE NETWORK MODEL FOR PREDICTING THE STOCHASTIC EFFECTS OF DISCONTINUOUS FIBRE COMPOSITES

**Lee T Harper, Thomas A Turner, Nicholas A Warrior**  
**The University of Nottingham**

**The School of Mechanical, Materials and Manufacturing Engineering**  
**University Park, Nottingham, NG7 2RD**

**Keywords:** *Directed fibre preforming, random, discontinuous, finite element*

## **Abstract**

*A random fibre network model is presented in conjunction with a novel finite element method to predict the tensile behaviour of random, discontinuous fibre laminates produced by a directed carbon fibre preforming (DCFP) process. Predictions from the model are compared against an analytical model and experimental data for a selection of studies, including the effect of fibre volume fraction, fibre length and virgin tow filament count on the tensile performance. The model is used to demonstrate the effects of increasing specimen thickness for different virgin tow sizes. A method is also presented to account for bundle fragmentation occurring during processing.*

## **1 Introduction**

Randomly reinforced discontinuous fibre composites are attractive for their relatively low manufacturing costs and rapid cycle times compared with textile-based systems. Historically, random fibre materials have suffered from low fibre volume fractions, poor consistency and low specific properties. Recent advancements in Directed Carbon Fibre Preforming (DCFP), have addressed some of these limitations [1], and mechanical properties are now approaching those of continuous, quasi-isotropic laminates [2]. With higher fibre volume fractions than conventional spray-up (~50% for random fibres) and the potential for fibre alignment, DCFP laminates are showing great promise for both semi-structural and structural applications.

The uptake of the technology into industry has been restricted by poor preform repeatability compared with textile systems. The use of inexpensive, high filament count rovings (>24K) has

been identified as the main cause of local volume fraction variation and high scatter in material properties [3]. This has previously limited the use of directed fibre preforms to semi-structural, cosmetic applications [4]. The detrimental effects of high filament count tows can be minimised, to a certain extent, by using shorter fibre bundles to improve macroscopic homogeneity [5]. In addition, a filamentisation technique has been developed to fragment the high filament count tows at the fibre chopping stage [1], to create low filament count bundles online from low cost, non-aerospace grade tows. Local volume fraction variations are reduced from  $\pm 15\%$  to less than  $\pm 5\%$  [5], whilst component costs are competitive at intermediate production volumes (1000-10,000ppa) [6].

A basic requirement for all new materials and processes is that they can be modelled and their performance predicted within reasonable limits. The main focus of this work is to study the influence of stochastic fibre coverage effects on the tensile properties of DCFP laminates. High bundle filament counts (>6K) and long fibre lengths (>23mm) are typically used within industrial DFP processes because they offer major cost savings and better preform rigidity during moulding. However, it is difficult to predict the mechanical performance of these coarse fibre mesostructures because of the high levels of heterogeneity caused by poor fibre coverage. Conventional analytical methods for random fibre composites use statistical averaging processes [7, 8] or classical laminate theory [9] to determine representative properties. A review in [3] has shown that these approaches do not adequately model the mesoscopic fibre architecture exhibited by DCFP. Stochastic variation induced by the fibre deposition process is overlooked and the filaments are assumed to be homogeneously distributed

throughout the laminate, rather than in bundle form. There is also no consideration for the scale dependency of the material, such as the effect of component thickness relative to the fibre bundle dimensions. In consequence, these models tend to over-predict the mechanical performance. Recent developments [10] have included adopting a fibre network approach in conjunction with laminate theory to investigate the mechanical property variation and specimen size effects for random chopped fibre laminates. Property variation is shown to decrease with increasing specimen thickness, decreasing filament count and decreasing fibre length. Representative Volume Elements (RVE) are shown to be a function of fibre length and can be of structural dimensions. This method accounts for stochastic fibre coverage variation, and stiffness predictions are shown to be within 10% of the experimental values. However, strength determination is limited because only the load carried by the fibre strands is taken into consideration. Stress concentrations within the matrix, caused by fibre ends or at fibre crossover points, are overlooked and the predicted strengths tend to be 25% too high.

## 2 Scope of paper

This paper presents a random fibre network approach in conjunction with a Finite Element Method (FEM). The random fibre network is used to investigate the heterogeneity induced during the fibre deposition stage and the FEM approach enables the fibres and resin to be modelled as distinct constituents, in order to remove the limitations imposed in [10]. A multi-scale approach is adopted to account for the complex meso-scale architecture and the effects of tow fragmentation. The model is used here to predict the tensile stiffness and strength for a range of fibre architectures. Of particular interest are the influence of parameters including fibre length, bundle filament count, fibre volume fraction and specimen thickness, all of which are known to affect the preform homogeneity [3, 5, 11]. Predictions from the model are validated using experimental tensile tests.

The performance of discontinuous, random composites is strongly influenced by the properties of the matrix material. This dependency is generally stronger than for fibre-dominated engineered fabrics, since the matrix is responsible for transferring the load between fibres through shear mechanisms at the bundle/matrix interface. The FE model can be used

to evaluate the use of toughened resins, in an attempt to improve the ultimate tensile strength of DCFP laminates. A range of epoxies with different post elastic responses are simulated using a continuum damage approach.

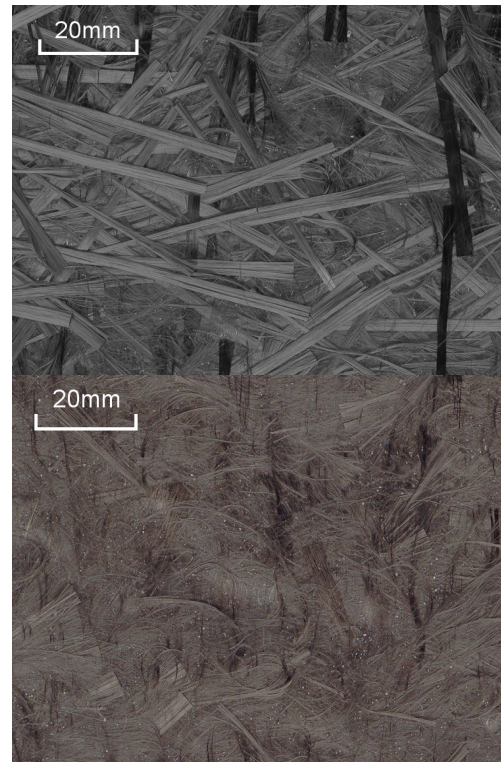


Fig. 1. Photographs of two 24K STS carbon preforms, with (bottom) and without (top) induced filamentisation.

## 3 DCFP material architecture

Carbon tows fragment as a result of the high velocity air stream used to deposit the tows onto the preform tool. Additional fragmentation can be typically induced in an attempt to provide homogeneous fibre coverage and to reduce the local areal mass variations associated with high filament count tows (see Fig. 1.) [1]. This phenomenon is difficult to control and a broad range of filament counts is often generated within each laminate, extending from single filaments through to the virgin tow size (24K). Reinforcement (filament or bundle) diameters within the model therefore cover several orders of magnitude which makes element selection difficult. This problem is also compounded by the fact that the unit cell is non-repeating and of structural size. An FE mesh that can accommodate a wide range of tow diameters is essential, but the resulting mesh density must not restrict the overall dimensions of the unit cell.

#### 4 Modelling concept

The current modelling strategy has been developed so that it can be universally applied to all random fibre materials. A process-specific simulation is used to generate the fibre network, since the spatial distribution of random fibres is largely dependent on the nature of the preforming/moulding process. The strategy currently in use simulates the fibre architecture at the mesoscopic level, using 1D beam elements in ABAQUS (type B22). Each beam is assumed to have a circular cross-section, where the diameter is a function of the filament count and tow volume fraction. Tow diameters are randomly assigned from a probability density function to reflect the mesostructure seen in experimental studies [11]. The matrix material is modelled using a regular array of 2D, plane stress continuum elements (type CPS8R). The beam elements are tied to the solid elements using the embedded element technique, a type of multi-point constraint within ABAQUS/Standard. The resulting fibre architecture is then passed to an intermediate solver interface to generate the meshes. An FE input deck is subsequently created and this is passed to ABAQUS/Standard for solution.

Random fibre networks have been generated using a DCFP process simulation, similar to the one described in [3]. Fibres are deposited over an area which measures two fibre lengths greater than the specified region of interest (ROI), in both the X and Y directions (see Fig. 2). Cartesian coordinates for the centroid of each tow are assigned randomly within the preform perimeter (outer rectangle, Fig. 2.) and a random orientation is generated between  $-\pi$  and  $\pi$ . The coordinates of the two fibre ends and the orientation are used to generate the intersections with the boundaries of the ROI (inner rectangle, Fig. 2.). Fibre deposition and cropping occur concurrently. A target fibre length within the ROI is determined from the laminate volume fraction and bundle dimensions. As each fibre is deposited, an algorithm checks for intersection with the ROI and then recalculates the fibre length if cropping is performed. A cumulative total of the fibre length within the ROI is used to establish if the volume fraction requirements have been met. This method ensures that both bridging and ending fibres are captured and that the volume fraction within the ROI is always as specified. It is assumed that fibres remain straight and that the position of each fibre is exclusive, allowing fibres to intersect. The coordinates for the fibre ends are written to a text

file ready for importing into the intermediate solver interface.

The random nature of the fibre distribution does not justify the use of periodic boundary conditions, since the unit cell is non-repeating. The following boundary conditions have been chosen to represent a conventional tensile test: The displacement along edge AB (see Fig. 2) is zero in both the X-direction and Y-direction. The displacement along edge CD is zero in the Y-direction and a uniform displacement is applied in the X-direction. A width of 25mm, a length of 120mm and a thickness of 3mm (unless otherwise stated) have been used to model the section of specimen located between the jaws of a conventional tensile test (BS2782-3).

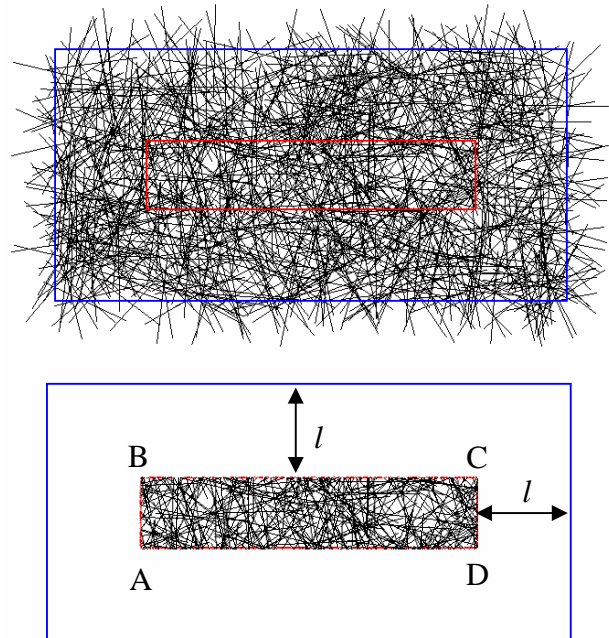


Fig. 2. Random fibre network generation. (Top) Fibres are deposited over an area which is two fibre lengths ( $2l$ ) greater than the specified ROI. (Bottom) Fibres are cropped to ROI boundary. Black lines represent the tow centre lines.

#### 5 Failure criteria and damage evolution model

Both constituent materials are assumed to be isotropic, therefore the Maximum Principal Stress failure criterion is considered to be suitable for predicting the damage onset. To simulate damage, it is necessary to evaluate the current stress state at each integration point within the model. If the stress state satisfies the failure criterion then the stiffness matrix of either the fibre or the matrix is degraded.

This degradation scheme has been programmed into two user-defined material subroutines (UMAT), one for each constituent, which are subsequently interfaced with ABAQUS. Fig. 3 shows a flow chart for the resin UMAT.

There are three possible scenarios: 1) undamaged, 2) damaged (post yield) and 3) damaged leading to fracture (final failure). The maximum and minimum Principal Stresses are calculated and are compared with the failure criterion to check for damage in tension and compression respectively. If no damage is present, then the stiffness matrix is calculated using the initial elastic constants (condition 1). However, if the yield point of the matrix is exceeded in either tension or compression ( $\sigma_{matrix}^t$  or  $\sigma_{matrix}^c$ ), then the onset of damage occurs. If the onset of damage is detected but the strain based failure criterion is not violated (condition 2), degradation factors are calculated to reduce the stiffness matrix. The rate at which the stiffness beyond the yield point is degraded is governed by either a tensile ( $d_t$ ) or compressive ( $d_c$ ) damage parameter. If  $d_t$ , for example, is close to zero then the matrix will demonstrate a brittle failure and the ultimate failure stress will coincide with the yield stress. The constant  $d_t$  or  $d_c$  is used to calculate the degradation factor ( $D$ ) in tension or compression respectively:

$$D = 1 - \frac{\left(\frac{\sigma_{\max}}{\sigma_{matrix}^t} - 1\right)}{d_t} \text{ or } 1 + \frac{\left(\frac{\sigma_{\min}}{\sigma_{matrix}^c} + 1\right)}{d_c} \quad (1)$$

$D$  is limited to a lower bound value of 1% for the direct stiffness components and 20% for the shear components [12]:

$$\begin{aligned} d_E &= \max(D, 0.01) \\ d_G &= \max(D, 0.2) \end{aligned} \quad (2)$$

Fracture or final failure is governed by a Maximum Principal Strain criterion. If the Principal Strain is exceeded then final failure occurs (condition 3) and the stiffness matrix is reduced by the maximum degradation factors. For this case, the Young's Modulus and shear modulus are degraded to 1% ( $d_E = 0.01$ ) and 20% ( $d_G = 0.2$ ) of their initial values respectively [12].

The stiffness matrix at the relevant integration point is recalculated as follows:

$$[C] = [S]^{-1} = \begin{bmatrix} \frac{1}{d_E E} & \frac{-\nu}{d_E E} & 0 \\ \frac{-\nu}{d_E E} & \frac{1}{d_E E} & 0 \\ 0 & 0 & \frac{1}{d_G G} \end{bmatrix} \quad (3)$$

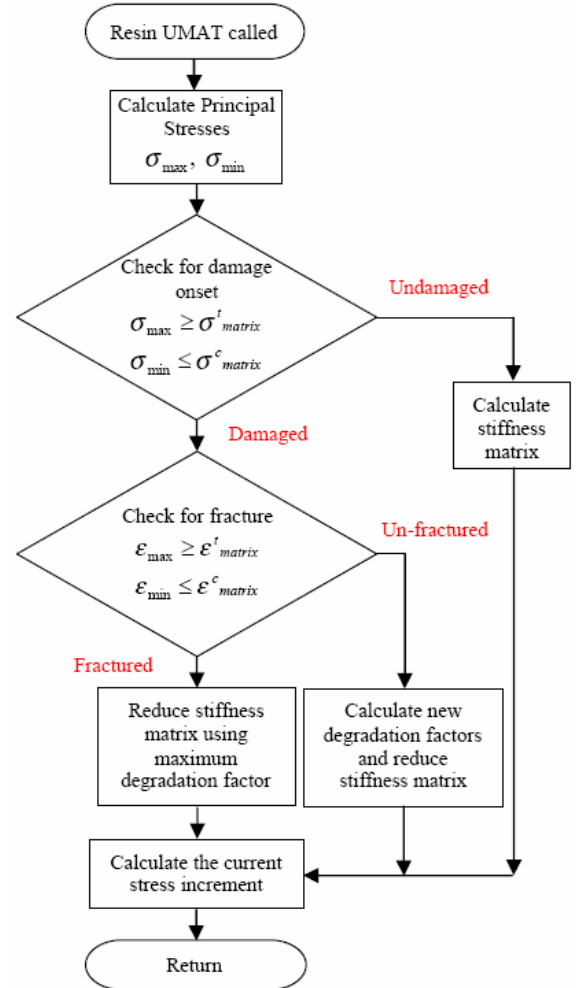


Fig. 3. Flow chart for the resin UMAT

The UMAT for the fibre is much simpler than for the resin, since  $S_{11}$  is the only relevant stress component for the beam elements. The fibres are assumed to be linearly elastic and the maximum or minimum value of  $S_{11}$  is used to determine whether the fibre fails in tension or compression respectively. Following failure, the longitudinal modulus at the integration point is reduced to 1% of the initial value.

A convergence study was performed to determine the mesh densities. Beam elements are 0.4mm long and resin elements are 0.2mm×0.2mm

throughout this study, based on the convergence of the elastic modulus for a 24K DCFP coupon. Table 1 shows the assumed material properties for the carbon bundles and two liquid epoxies. The tow properties are calculated from the rule of mixtures (assuming a 60% tow  $V_f$ ) using manufacturers data for Toho Tenax STS carbon fibre. Resin values were determined experimentally for DLS1692, a low cost development epoxy supplied by Hexcel. The toughened epoxy is a theoretical material higher strain to failure but similar ultimate tensile strength to DLS1692. The damage model has been used to simulate representative stress/strain curves for the two matrix systems, (see Fig. 4), using a square model consisting of 1000 resin only elements.

Table 1. Constituent properties

	Carbon Tow	DLS1692 Epoxy	Toughened Epoxy
$E_{11}$ (GPa)	137	3	3
$\nu_{12}$	-	0.38	0.38
$\sigma^t$ (MPa)	2650	60	10
$\sigma^c$ (MPa)	1450	250	250
$\epsilon^t$ (%)	-	2	4.5
$d_t=d_c$	-	0.001	15

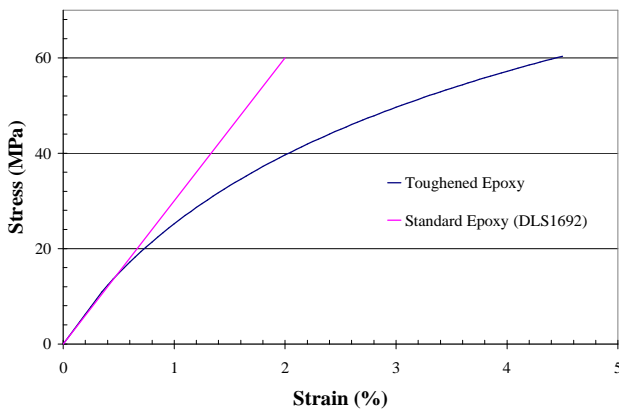


Fig. 4. Stress/strain curve for two cured epoxy resins

Generally there is good agreement between the FE model and the experimental data. A representative stress/strain curve is presented in Fig. 5 for a 6K DCFP material. The initial elastic stiffness and the ultimate strength predictions are within 5.4% of the numerical average of the nine tensile specimens. It is clear that failure occurs catastrophically and that the specimens are generally of a brittle nature. However, the onset of damage starts before the final failure for both the experimental and theoretical curves. It was noted that there was audible resin cracking during the

latter stages of the experimental test. Damage plots from the FE model show that the onset of failure occurs in the matrix at a strain of 0.004. The influence of this progressive matrix damage appears to have been captured by the continuum damage model, since both stress/strain curves are in close agreement. Damage plots at the end of the simulation are presented in Fig. 6 for both the resin and fibre elements. There is clearly a damage zone where both element types have failed, which passes from one side of the specimen to the other. Smaller damage zones are present elsewhere in the matrix material, but these are isolated regions. At the damage onset point (0.4% strain) a number of small local regions of damage form in the matrix. As the applied strain increases some of these regions coalesce and join together. For the current case, the damage in the matrix progresses across the width of the specimen. As the resin elements fail, load is redistributed amongst the neighbouring fibres until the stress-based failure criterion is violated. Failure of the fibres across the damage zone is synchronised, which results in a sudden, catastrophic failure.

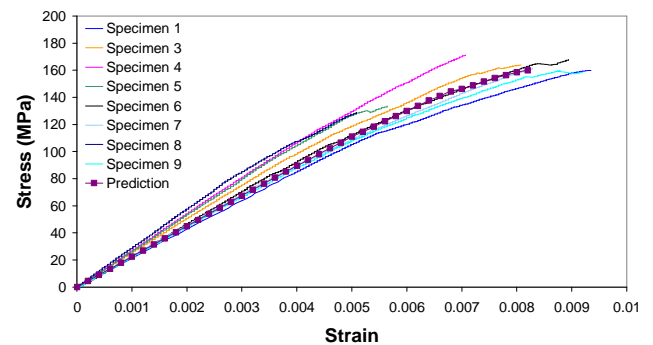


Fig. 5. Comparison of stress/strain curves for 9 experimental tensile specimens and 1 simulation.

The fibre architecture comprised 3K non-filamentised bundles, 23mm in length at 27% fibre volume fraction.

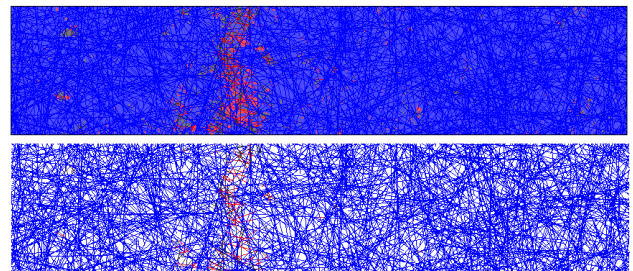


Fig.6. Final damage plot in the matrix (top) and fibres (bottom) for the predicted curve from Fig. 5.

It is important to note the level of variation in the experimental results for this material, figures of

up to 45% have been reported [3]. Where computational resources allow, 10 simulations have been conducted for the scenarios presented in subsequent sections of this paper, and these have been validated by the same number of experimental tests.

## 6 The effect of tow filament count

Low filament count tows yield higher laminate stiffnesses and strengths because of the improved level of macroscopic homogeneity. Unreinforced regions are considerably smaller with lower filament count tows [11], and therefore the number of detrimental stress concentrations is reduced. Fig. 7 shows a comparison of the stress/strain curves for two different filament counts. The 3K material exhibits a characteristic brittle failure which is dominated by the fibres, whereas the 24K material shows a more progressive failure type dominated by the matrix. The 24K laminate is highly dependent on the matrix material for the transfer of load between the fibres, because of the high concentration of resin rich areas. Conversely, the 3K laminate encounters a greater number of fibre-fibre contacts per unit length. Load sharing can occur at the fibre cross-over points, reducing the local strain in the matrix material.

Fig.8. shows the effect of increasing tow filament count on the tensile modulus. The FE model is compared with a multi-scale, analytical solution from [11] and with experimental data from [13]. Both models generally over predict the mean experimental values by 20-40%, but there is a much closer agreement between the FE model and the maximum experimental values in each case. The FE predictions are generally within 10% of the experimental maximums, with the closest agreement for the small filament counts. The experimental preforms were produced on the directed fibre preforming machine at the National Composites Centre, Dayton, Ohio, which is not optimised for processing carbon. Areal mass variations of up to 15% have been reported for this facility [3] and the fibres can also become preferentially aligned in the 90° direction due to the fibre chopping apparatus.

There is close agreement (3%) between the two predictive models for small tow sizes of 1K, but this error increases to 11% as the tow size increases from 1K to 12K. The accuracy of the analytical model is limited for high filament count materials because it does not account for local variations in preform areal mass; in particular it neglects the large resin rich

regions which are common for high filament count laminates. This is the major advantage of the random fibre network approach currently used to generate the fibre distributions for the FE model.

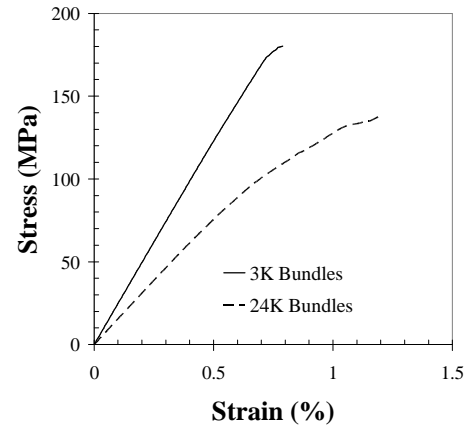


Fig.7. Stress/strain curves for two DCFP plaques of identical fibre length (23mm) and fibre volume fraction (30%) but different tow filament counts.

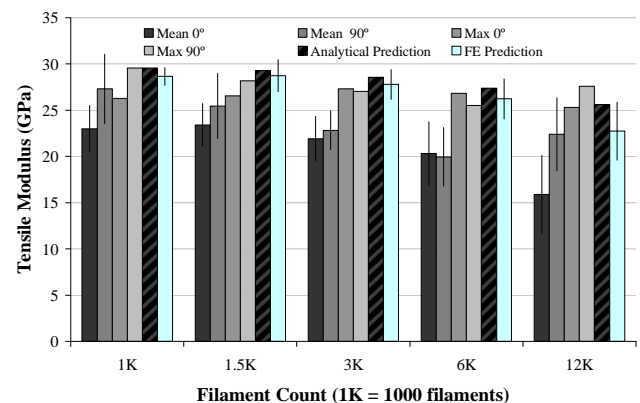


Fig.8. The effect of increasing tow filament count on the tensile modulus. Experimental preforms were manufactured on the DCFP machine at the NCC, Dayton, Ohio [13].

Inducing tow filamentisation has proven to be a successful method for increasing both the tensile stiffness and strength when utilising high filament count bundles [11], particularly for structures where the diameter of the fibre bundles is similar to the thickness of the laminate and the level of heterogeneity is high. With such notable increases in performance it is vital that a filamentised architecture can be generated by the random fibre network model. The use of beam elements has proven to be an economical way of representing the fibre bundles, without restricting the capabilities of modelling large volumes of material. This concept has been extended for producing filamentised architectures, using variable section diameters for

each beam element. Fig.9. shows a range of theoretical curves representing different levels of induced filamentisation, which have been generated according to Eqn. 4:

$$y = \sin^{\beta-1} \left( \frac{x\pi}{2K} \right) \quad (4)$$

where  $K$  is the virgin tow size,  $\beta$  is the filamentisation factor,  $x$  is the fragmented bundle filament count and  $y$  is the frequency.

The model generates a random frequency value between 0 and 1 and the filamentisation function returns a corresponding fragmented filament count between a single filament and the virgin tow size. The filamentisation function returns unfilamentised bundles as  $\beta$  tends to infinity, and decreasing bundle sizes as  $\beta$  decreases towards unity. Experimental observations confirm that laminates typically contain some virgin tows which have resisted fragmentation at high levels of filamentisation. This is reflected in the shape of the filamentisation curves presented in Fig.9, which converge at a frequency of 1.

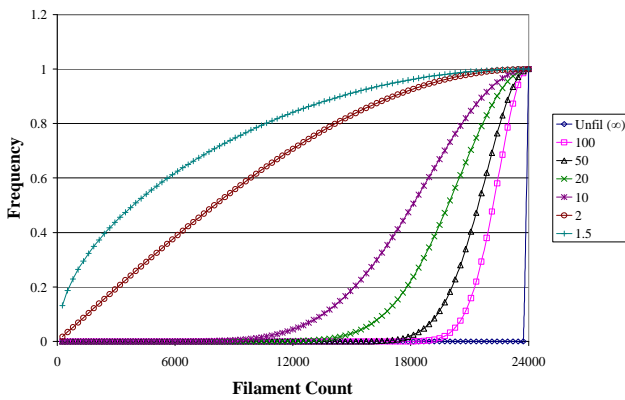


Fig.9. A selection of frequency charts generated using a sine function to model increasing levels of induced filamentisation.

Fig.10. shows a comparison of two simulated fibre architectures for filamentised and non-filamentised bundles. The fibre volume fraction is identical in each case for this 25x25mm representative sample, but the number of fibre segments increases from 138 to 247 when  $\beta$  is reduced from  $\infty$  to 1.5. The filament count of each bundle is depicted by the width of the bundle and by using a grey scale value (black representing the virgin filament count and white single filaments, with red centre lines). The large white, resin rich regions in the unfilamentised sample (left) are divided into smaller regions by the presence of

lower filament count bundles in the filamentised plaque (right). This reduces the magnitude of the stress concentrations caused by these unreinforced areas and provides improved local load sharing between neighbouring fibres.

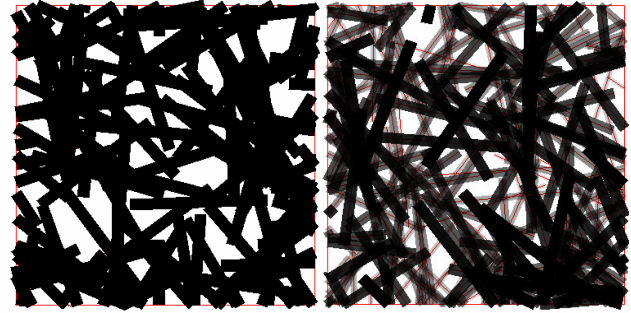


Fig.10. Two screen shots from the process model showing the effects of inducing filamentisation. (Left)  $\beta=\infty$  (Right)  $\beta=1.5$

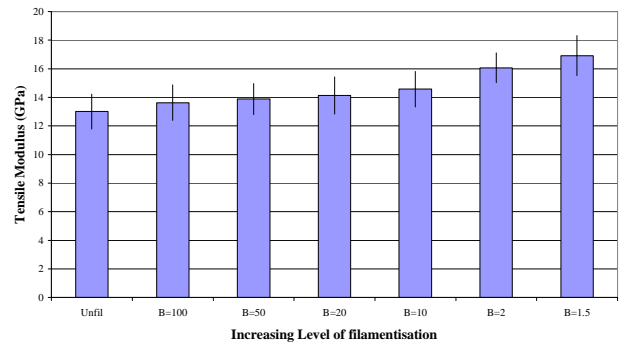


Fig. 11. Effect of increasing the level of induced filamentisation on the tensile stiffness.

The influence of increasing the level of filamentisation is presented in Fig. 11 for the tensile stiffness. A 30% increase in stiffness is achieved by reducing the  $\beta$  value from  $\infty$  to 1.5. This percentage increase is representative of the increase in stiffness reported in [11] for a similar material. Comparative experimental data is limited at this time because the exact level of filamentisation is unknown. Work continues to develop a reliable method for determining the tow filament count distribution of laminates subjected to variable levels of induced filamentisation.

### 7 The effect of fibre length

Fibre length is an important parameter for both the quality of the preform and for the mechanical performance of the moulded component. Short fibres present problems with preform handling, but conversely help to improve the macroscopic coverage issues that cause poor mechanical

properties when processing high filament count tows. A study in [5] showed that an increase in mechanical performance was achieved for increasingly shorter fibre lengths (down to a critical value). However, it was noted that this trend resulted because the effects of fibre length were not studied in isolation, since the tow filament count reduced with decreasing fibre lengths (natural filamentisation). The advantage of the current modelling approach enables variables to be easily studied in isolation. The model is used here to generate stiffness and strength trends as a function of fibre length only. Simulations are validated against experimental tensile tests, using carbon fibres with a low tendency for natural fragmentation. The minimum fibre length is limited to 23mm however, in order to prevent the occurrence of natural filamentisation.

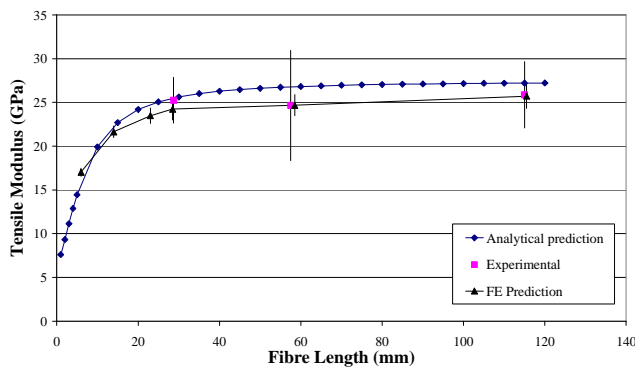


Fig. 12. The effect of increasing fibre length on tensile modulus (6K bundles, 30%  $V_f$ , 3mm laminate)

Fig. 12 shows a comparison between the analytical model [11], the FE model and the experimental results. There is excellent agreement between the FE and experimental results, with a maximum error of less than 4%. The two models are in close agreement for shorter fibre lengths (<15mm), but the analytical solution tends to over-predict for longer fibre lengths as the level of heterogeneity in the preform increases. The analytical model generally over predicts the experimental data by 10% for the range of fibre lengths tested. Both the FE model and the experimental results therefore demonstrate that longer fibres yield higher tensile stiffness up to a critical point, beyond which the stiffness is shown to plateau.

Fig. 13 shows a comparison of the experimental tensile strength results with the FE predictions. Predictions for both the 28.75mm and

57.5mm fibre lengths are within 2.5% and 6.0% of the experimental results. Simulations for the 115mm fibre length over predict the tensile strength by 37%. This can be partly attributed to low experimental values caused by increasing fibre curvature for longer fibre lengths. Secondly, this error can be attributed to the simplified fibre failure mechanism currently employed by the model. Load is only transmitted axially along the bundle because of the nature of beam elements. Therefore, local failure initiation points, typically caused by transverse bundles, are not accounted for with this model.

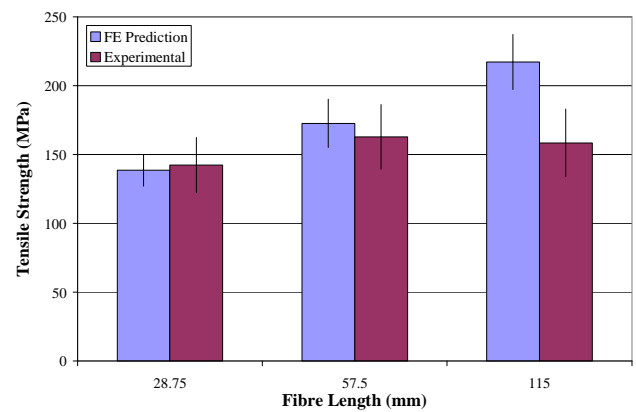


Fig. 13. The influence of increasing fibre length on tensile strength (6K bundles, 30%  $V_f$ , 3mm laminate)

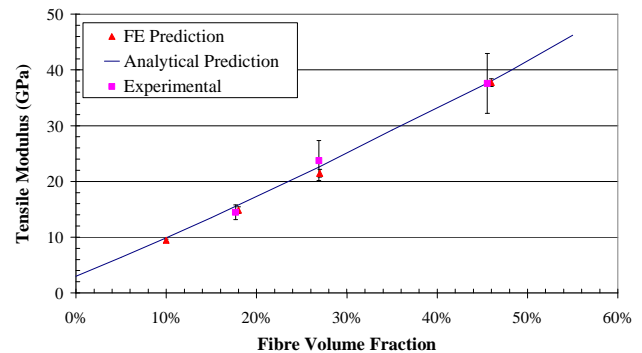


Fig. 14. The effect of increasing fibre volume fraction on the tensile stiffness of 3mm laminates comprising 3K bundles

### 8 The effect of fibre volume fraction

The effect of increasing the fibre volume fraction on tensile stiffness is shown in Fig. 14, for a range of typical DCFP production values. The analytical model from [11] is used to assess the quality of the stiffness predictions generated by the FE model. There is excellent agreement between the two predictive models and the experimental data. The FE model is within 9% of the experimental data

for a  $V_f$  of 30% and within 3% for the other experimental points. A major advantage of the FE model over the analytical type is the ability to predict the magnitude of potential property variation. The error for the experimental points ranges from 9% to 15%, whereas the error predicted by the FE model is less than 4% in each instance. Currently, no process induced effects are taken into consideration by the fibre network generator, since the fibre distributions created are uniformly random. In [3] it was established that the fibre deposition strategy, the height of the chopping apparatus and the robot speed all affect the quality of the preform, creating varying levels of areal mass variation. This oversight is likely to contribute to the low standard deviation bars in Fig. 14, compared with the experimental data.

### 9 The effect of component thickness

Historically, components made by directed fibre preforming have typically been less than 5mm thick, in the form of closure panels for the automotive industry or secondary aircraft structures. There is a growing need for thicker components due to the increasing structural demands placed on DCFP. Current filamentisation strategies make it difficult to produce thick parts because inefficient fibre packing restricts the ceiling volume fraction, creates problems with preform loft and reduces preform permeability by an order of magnitude. Experimental results in [3] indicate that greater levels of homogeneity are achievable with thicker components. Tensile stiffness and strength were shown to increase by 8% and 25% respectively when the specimen thickness was increased from 1.8mm to 4mm. These results are supported by predictions from the FE model in Fig. 15. The tensile stiffness increases sharply for increasing thicknesses between 0.5mm and 5mm, after which the stiffness converges towards a value of 25GPa. The 6K curve appears to converge earlier than the 24K curve because of the relative scale of the reinforcement to the laminate thickness. Clearly, high filament count tows can be used without the need for filamentisation, providing the specimen thickness is high. The model can therefore be used to intelligently choose the tow filament count, the level of filamentisation required and the component thickness, in order to yield the desired mechanical properties.

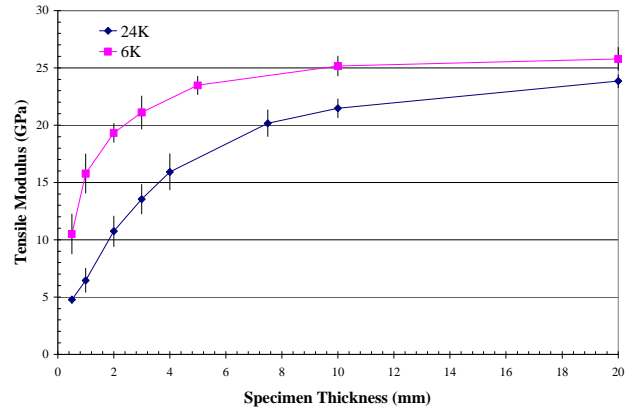


Fig. 15. Effect of increasing specimen thickness for two tow sizes, but constant laminate  $V_f$ .

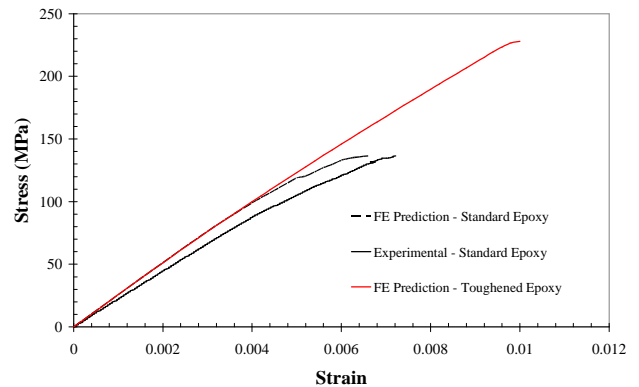


Fig. 16. Effect of using a toughened epoxy over a standard epoxy resin on the ultimate tensile strength.

### 10 The effect of resin toughness

The performance of random, discontinuous composites is strongly influenced by the mechanical properties of the matrix material. This dependency is considerably stronger than that seen in textile composites, because the matrix is required to transfer the applied load to the fibres through shear mechanisms at the fibre/matrix interface. This study investigates the use of two different matrix systems, where the uniaxial stress/strain curves for each resin are shown in Fig. 4. Fig. 16 shows the stress/strain behaviour for a composite (6K tows, 28mm long, 30%  $V_f$ ), utilising the two different resins. Both resins have identical initial elastic moduli and identical ultimate strengths. However, the increase in strain to failure between the standard resin (2%) and the toughened resin (4.5%) increases the ultimate tensile strength of the composite by over 66%. There is very good agreement between the FE prediction and the experimental stress/strain curve for the standard, brittle epoxy. No experimental data is currently available for a toughened system. The model indicates that adding a suitable toughening

agent to an epoxy resin, such as rubber particles or a thermoplastic, can have a positive effect on the ultimate tensile properties of random fibre laminates.

## 11 Conclusions

A random fibre network model has been presented along with an FE method for predicting the tensile behaviour of discontinuous fibre composites, for both random and aligned architectures. The model has been used to study the effects of the fibre architecture on the tensile properties of DCFP. Comparisons with a conventional analytical stiffness model have highlighted the advantages of the random fibre network approach. The major benefit is that the model can account for the effect of high levels of heterogeneity typically encountered with discontinuous, high filament count bundles. The stochastic effects of the material architecture are also considered, making it possible to determine confidence levels for the predicted mechanical properties. The model has been used to successfully isolate the effects of decreasing fibre length and decreasing tow filament count, which has not always been possible with experimental characterisation programmes. A method for generating filamentised fibre architectures has been developed, which enables a wide range of tow filament counts to be modelled within the same laminate, from single filaments to virgin bundles, without restricting the global volume of the model. This part of the model is currently awaiting experimental validation.

The model shows very good agreement with the available experimental data, in terms of predicting the stress/strain response, and also the ultimate properties. The model has been used to demonstrate the negative effects of using inexpensive, high filament count tows on the tensile properties, but also the benefits of using high velocity air to fragment some of the fibre bundles into smaller filament groups. The need for fibre filamentisation is reduced as the thickness of the laminate increases, even for high filament count bundles. The importance of selecting a fibre architecture to suit the intended application has been highlighted and the model can be used to perform parametric studies for material optimisation. Finally, the model has been used to determine the effects of using a toughened resin. Increasing the strain to failure of the matrix material has a positive effect on the UTS of the random fibre laminate.

## 12 References

- [1] Harper, L.T., T.A. Turner, N.A. Warrior, and C.D. Rudd Automated preform manufacture for affordable lightweight body structures. in *26th International SAMPE Europe Conference*. 2005. Paris.
- [2] Harper, L.T., T.A. Turner, N.A. Warrior, and C.D. Rudd Low cost carbon fibre-based automotive body panel systems. in *27th International SAMPE Europe Conference*. 2006. Paris.
- [3] Harper, L.T., T.A. Turner, N.A. Warrior, J.S. Dahl, and C.D. Rudd, *Characterisation of random carbon fibre composites from a directed fibre preforming process: Analysis of microstructural parameters* Composites Part A: Applied Science and Manufacturing, 2006. 37(11): p. 2136-2147.
- [4] Chavka, N.G., J.S. Dahl, and E.D. Kleven F3P fiber preforming for the Aston Martin Vanquish. in *SAMPE Europe International Conference*. 2001. Paris.
- [5] Harper, L.T., T.A. Turner, N.A. Warrior, and C.D. Rudd, *Characterisation of random carbon fibre composites from a directed fibre preforming process: Effect of fibre length* Composites Part A: Applied Science and Manufacturing, 2006. 37(11): p. 1863-1878.
- [6] Turner, T.A., L.T. Harper, N.A. Warrior, and C.D. Rudd, *Low cost carbon-fibre based automotive body panel systems - a performance and manufacturing cost comparison* Submitted to Journal of Automobile Engineering - Proceedings of the Institution of Mechanical Engineers Part D, 2006.
- [7] Christensen, R.M. and F.M. Waals, *Effective stiffness of randomly oriented fibre composites* Journal of Composite Materials, 1972. 6: p. 518-532.
- [8] Pan, N., *The elastic constants of randomly oriented fiber composites: A new approach to prediction* Science and Engineering of composite materials, 1996. 5(2): p. 63-72.
- [9] Halpin, J.C. and N.J. Pagano, *The laminate approximation for randomly oriented fibre composites* Journal of Composite Materials, 1969. 3: p. 720-724.
- [10] Ionita, A. and Y.J. Weitsman, *On the mechanical response of randomly oriented reinforced chopped fibre composites: Data and model* Composites Science and Technology, 2006. 66(14): p. 2566-2579.
- [11] Harper, L.T., T.A. Turner, N.A. Warrior, and C.D. Rudd, *Characterisation of random carbon fibre composites from a directed fibre preforming process: The effect of tow filamentisation* Composites: Part A: Applied Science and Manufacturing, 2007. 38(3): p. 755-770.
- [12] Blacketter, D.M., D.E. Walrath, and A.C. Hansen, *Modeling damage in a plain weave fabric-reinforced composite material* Journal of Composites Technology and Research, 1993. 15(2): p. 136-142.
- [13] Dahl, J.S., G.L. Smith, J.E. Devries, D.Q. Houston, S. Iobst, and L. Berger The influence of fiber tow size on the performance of chopped carbon fiber reinforced composites. in *37th International SAMPE Technical Conference*. 2005. Seattle, WA.